Macromolecules

Article

pubs.acs.org/Macromolecules

Kinetics and Mechanisms of Radical-Based Branching/Cross-Linking Reactions in Preformed Polymers Induced by Benzophenone and Bis-Benzophenone Photoinitiators

Nicholas D. Carbone, Madalina Ene, Jeffrey R. Lancaster, and Jeffrey T. Koberstein*

Departments of Chemistry and Chemical Engineering, Columbia University in the City of New York, 500 West 120th Street, New York, New York 10027, United States

Supporting Information

ABSTRACT: The general mechanism for photo-cross-linking of preformed polymers is studied by comparing the efficacy of monofunctional benzophenone (BP) and bifunctional bis-benzophenone (BP-BP) photoinitiators for inducing radical chain branching reactions in glassy polystyrene (PS) and rubbery poly(*n*-butyl acrylate) (P*n*BA). Upon UV irradiation, macroradicals form and initiate a variety of cross-linking and scission reactions. The kinetics and mechanisms of these macroradical reactions were monitored by gel permeation chromatography (GPC) measurements of changes in the polymer molecular weight distributions. Molecular weight increases are associated with chain branching while decreases in molecular weight are indicative of chain scission. We study the early stages of radical recombination where branching is manifest as the formation of three- and four-arm star polymers that are soluble and can be detected/differentiated by GPC. Branching is observed even in glassy PS; however, the reactions are much faster in rubbery P*n*BA, consistent with the expected influence of main chain mobility. At equal chromophore equivalents, BP-BP was found to be more efficient than BP for producing macroradicals, primarily due to a lower degree of self-quenching in BP-BP. When added to glassy PS, the higher efficiency of BP-BP did not translate into more chain branching, except at high additive concentration where the probability of BP-BP chain bridging reactions becomes significant, but instead led to a higher degree of main chain scission. The latter result was attributed to the larger distance between chromophores for BP-BP than for BP at equal benzophenone equivalents. In marked contrast, almost no main chain scission was found for either additive in P*n*BA, and BP-BP proved more effective for promoting chain branching. The susceptibility to main chain scission is found to be dependent upon the location of radical formation by hydrogen abstraction from the polymer. In PS, radicals can form on the chain backbone, and radical scission reactions lead to fragmentation of the polymer chain. In P*n*BA, radicals form preferentially on the pendant side chains, and radical scission reactions do not lead to main chain breakage. A simple probability-based model was found to capture the salient features of radiation-induced branching in preformed polymers.

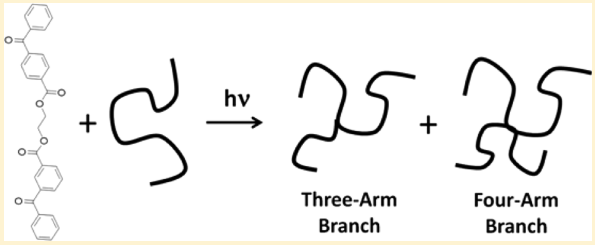

INTRODUCTION

Cross-linking, to promote either chain branching or network formation, is a common method for polymer modification because of its profound influence on mechanical properties and characteristics such as mobility, solubility, and diffusion. Covalent cross-links are usually introduced during polymer synthesis by the incorporation of multifunctional monomers or cross-linking agents. The resultant materials are thermoset polymers that retain the shape in which they were polymerized and are insoluble in all solvents. Polymers may also be cross-linked after synthesis by the addition of a cross-linking additive,[1] by exposure to high-energy radiation,[2,3] or by a combination of the two processes. Additives that cross-link upon heating include sulfur (i.e., vulcanization),[4,5] peroxides,[6,7] and glutaraldehyde, a common fixative for proteins.[8−13] Radiative methods are typically based on the formation of radicals by exposure to high-energy radiation such as γ-rays and electron beams. Alternatively, photo-cross-linking of preformed polymers can be achieved by use of a photoinitiator that forms radicals upon exposure to visible or UV radiation. The photoinitiator can be attached to the polymer during synthesis[14,15] or can be an additive.[16−18] The excited photoinitiator generally abstracts a hydrogen atom from the polymer to form a macroradical. Covalent cross-links form when two macroradicals annihilate by recombination. A macroradical can also undergo main chain scission by β-scission, a process that decreases the molecular weight.

Benzophenone and its derivatives are perhaps the most widely used photoinitiators and have been studied extensively, both as additives[16,17,19−21] and incorporated into functional polymer side chains.[22,23] Most recently, bifunctional bis-benzophenone compounds have been used to induce photo-cross-linking in preformed polymers[16,24,25] and have been shown to be effective even for cross-linking polymer glasses.

Received: April 8, 2013
Revised: June 4, 2013
Published: July 3, 2013

In this paper we examine the general mechanism of photo-cross-linking in preformed polymers by comparing the relative efficiencies and mechanistic differences between BP and BP-BP as photoinitiators for radical-induced branching/grafting reactions. Because the efficiency of radical branching reactions may be a strong function of mobility, two different polymers are studied: polystyrene (PS), a glass at room temperature, and poly(*n*-butyl acrylate) (P*n*BA), a rubber at room temperature. Gel permeation chromatography measurements of the polymer molecular weight distributions are used to track branching and other radical induced reactions in the two polymers when exposed to ultraviolet (UV) radiation in the presence of one of the photoinitiators.

EXPERIMENTAL SECTION

Materials. Polystyrene (PS) (M_n = 46 000, PDI = 1.03) was purchased from Waters Associates. Two poly(*n*-butyl acrylate) samples were purchased from Polymer Source, Inc.: P*n*BA1 (M_n = 60 000, PDI = 1.08) and P*n*BA2 (M_n = 43 000, PDI = 1.08, Polymer Source, Inc.). HPLC-grade toluene (Pharmco-Aaper) and benzophenone (BP) (Fischer Scientific) were used as received. The bifunctional bis-benzophenone adduct (BP-BP) shown in Figure 1 was synthesized following the method reported previously.[16] The final material (fraction A, see Supporting Information) used was a mixture of meta−meta, meta−para, and para−para functionalities such that the ratio of meta:para was 1:3.

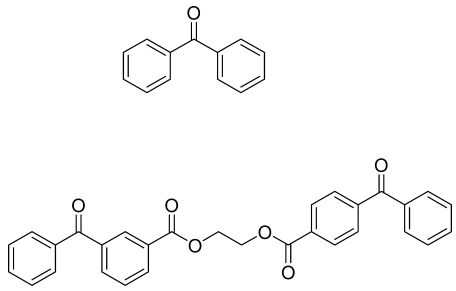

Figure 1. Structure of the benzophenone (BP), top, and *α-m-,β-p*-bis-benzophenone (BP-BP), bottom, photoinitiators.

Substrate Preparation. Silicon wafers (Wafer World, Inc.) were cut into 1 cm by 1 cm squares and placed in piranha solution (3:1 H_2SO_4:H_2O_2; *caution: piranha solution is extremely dangerous*) overnight. Wafers were washed first in DI H_2O and then in ethanol and were subsequently dried with N_2 in a clean hood. After treatment in a UV-ozone cleaning system (UVOCS, Inc.) for 20 min, the wafers were again washed in DI H_2O and ethanol and dried with nitrogen in a clean hood. The cleaning procedure removes all organic contaminants and produces a fresh oxide layer on the silicon wafer.

Solution Preparation. Solutions of 20 mg/mL PS and P*n*BA1 in toluene were agitated with a vortexer for 30 min and split into nine scintillation vials containing approximately 0.5 mL of solution each. One vial was set aside as a control. BP was added to four vials in molar ratios of 32:1, 8:1, 2.4:1, and 1:1, while BP-BP was added to the last four vials in molar ratios of 16:1, 4:1, 1.2:, and 0.5:1. The molar ratios for BP-BP were kept at half those of BP to keep the number of benzophenone equivalents equal in the two systems. P*n*BA2 solutions of 32:1 and 16:1 molar ratios of BP and BP-BP, respectively, were also prepared.

Sample Preparation. Slow evaporative solution casting produced a polymer/BP film with visible phase separation and crystallization (see Supporting Information). Films containing the photoinitiators were therefore formed by rapid spin-coating (Laurell Technologies Co., WS-400A-6NPP/LITE; 2000 rpm; 1 min) onto silicon wafers from a mutual volatile solvent to freeze in a dispersed morphology. The asymmetric structure of BP-BP, a *p*-benzophenone and a *m*-benzophenone, reduces its ability to crystallize, but its larger size renders it less miscible in the polymer matrices in comparison with BP. Annealing the samples after spin-coating led to phase separation and crystallization in both the BP and BP-BP systems; however, phases and or crystals could not be detected by optical microscopy directly after spin-coating. Samples were therefore irradiated immediately after spin-coating to minimize any segregation effects. Aggregation and phase separation at scales below the detection limit of optical microscopy are still feasible and would be favored in the BP systems. The film thicknesses measured by ellipsometry (alpha-SE, J.A. Woolam, Co.) were 128 ± 6 nm for PS and 110 ± 29 nm for P*n*BA. PS and P*n*BA1 samples were irradiated with a 350 nm ultraviolet source (UVP, Inc., 200 $\mu W/cm^2$) under an argon blanket in quartz-topped chambers for 0 min (control), 30 min, 60 min, 90 min, 3 h, 4.5 h, 6 h, 7.5 h, and 9 h. P*n*BA2 was prepared in the same manner as P*n*BA1 and irradiated for 0 min (control), 1 min, 5 min, 10 min, 15 min, 20 min, 25 min, 30 min, 40 min, 50 min, and 1 h. The source was run for 30 min before the start of each experiment to eliminate startup transients. Specimens were irradiated on a rotating stage to optimize the spatial homogeneity of irradiation.

GPC Analysis. After irradiation, specimens (i.e., films on cut silicon wafers) were stored in scintillation vials in a dark drawer to eliminate the possibility of further reactions. No differences in GPC response were observed between a fresh specimen and a specimen stored in this fashion for 5 days, confirming the appropriateness of this storage method. EPR analysis showed no measurable extant radicals in the system postirradiation. Solutions for GPC analysis were prepared by placing 0.200 mL of HPLC toluene in each vial and followed by shaking on a vortexer for 30 min. 0.05 mL of a 1 mg/mL solution of 2350 Da PS in tetrahydrofuran was added as an internal standard subsequent to the shaking. Solutions were then filtered through a 0.2 μm PTFE syringe filter and injected into the GPC (two Polymer Laboratories' ResiPore columns in a Shimadzu HPLC system: LC-10ATvp pump, CTO-10ACvp column oven, SPD-10a UV−vis detector, RID-10A RI detector, SCL-10Avp system controller, and a Wyatt miniDAWN TREOS static light scattering detector). Analysis was performed using custom MATLAB programs and Origin 8.0. Molecular weights were confirmed using a Wyatt miniDAWN light scattering detector (PS d*n*/d*c*: 0.185 mL/g; P*n*BA d*n*/d*c*: 0.08 mL/g). d*n*/d*c* was measured using Wyatt miniDAWN in batch mode at 657 nm as well as Brookhaven Instruments differential refractometer (BI-DNDCW) at 535 nm to determine wavelength dependence. GPC data were calibrated using linear PS standards (EasiVial PS-M(2 mL), Varian). Absolute P*n*BA molecular weights were determined from the PS calibrated values by correcting for hydrodynamic volumes using tabulated Mark−Houwink constants.[26]

RESULTS

The efficacies of benzophenone (BP) and bis-benzophenone (BP-BP) as photoinitiators to induce radical branching reactions in preformed polymers were studied for polystyrene (PS), a glass at room temperature, and poly(*n*-butyl acrylate) (P*n*BA), a rubber at room temperature. Chain branching was monitored by applying gel permeation chromatography (GPC) to measure changes in the molecular weight distribution (MWD) upon UV irradiation in an inert atmosphere. Control specimens, prepared without photoinitiators, showed no changes in MWD after 9 h of UV irradiation (see Supporting Information), indicating that oxygen had been effectively excluded and that the UV wavelengths used did not degrade the polymers without added photoinitiators. Any changes in the MWD of polymers to which the photoinitiators have been added can therefore be attributed solely to the effects of the photoinitiators.

The plausible mechanisms of photochemically induced macroradical formation and main chain scission in BP and BP-BP are identical as shown in Figure 2. The macroradical cross-linking reactions of BP and BP-BP are compared in Figure 3. The branching reactions are identical for the two photoinitiators except for the additional bridging mechanism that couples two

dx.doi.org/10.1021/ma4007347 | *Macromolecules* 2013, 46, 5434−5444

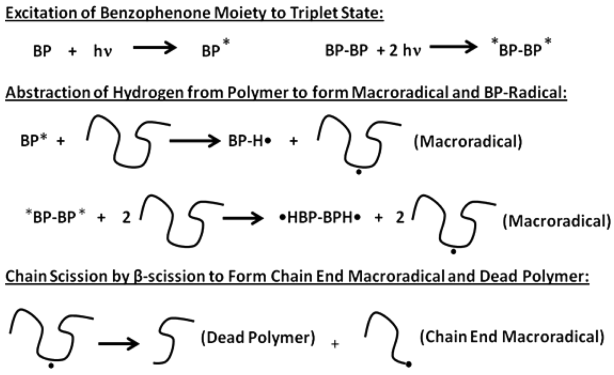

Figure 2. Photochemically induced radical reactions of BP and BP-BP leading to the production of macroradicals. BP-BP excitation and radical reactions occur one excited state or photon at a time with no required correlation.

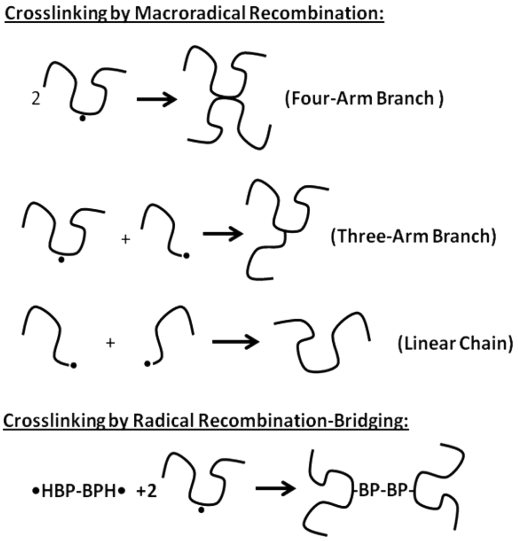

Figure 3. Schematic description of macroradical branching reactions, including the radical recombination-bridging reaction unique to bifunctional BP-BP.

macroradicals by virtue of a BP-BP bridge, a reaction that is not possible for the monofunctional BP system. The two photoinitiators also have an intrinsically different spatial distribution of photoactive benzophenone moieties because two benzophenone moieties are linked together in one BP-BP molecule. The spatial distribution of radicals formed may therefore be different for the two photoinitiators, a factor that may lead to differences in branch structure and branching efficiency.

The effects of UV exposure on the MWDs of glassy PS containing BP and BP-BP are shown in Figure 4. Two parameters were studied in these experiments: the total time of UV exposure and the equivalents of photoinitiator added. The equivalents of photoinitiator added is defined as the number of benzophenone moieties added per polymer molecule. The concept of equivalents is adopted because one BP-BP molecule contains two benzophenone moieties, whereas one BP molecule contains only one. Samples with equal equivalents of BP and BP-BP added then contain an equal number of benzophenone moieties per polymer molecule.

The chromatograms for PS exhibit both increases and decreases in MW upon UV exposure, indicating that BP and BP-BP are capable of inducing radical-based chemical reactions even in the glassy state. Increases in molecular weight can be attributed to radical-induced branching/grafting reactions while decreases in molecular weight arise from main chain scission reactions. The major peak centered at around 400 monomers is associated primarily with PS chains that have not undergone radical reactions and accounts for a large fraction of the chromatogram, demonstrating that only a small fraction of the PS chains undergo radical reactions under these conditions. The chromatograms as a function of exposure time and those for different photoinitiator equivalents can be superimposed, illustrating that an increase in photoinitiator content has the same effect as increasing the UV exposure time. The increase in higher molecular weight branched polymers brought about by addition of BP and BP-BP is roughly the same, indicating at least qualitatively that the amount of radical branching is primarily dependent on the number of photoinitiator equivalents and not so much on the nature of the photoinitiator molecule. The polymers with increased molecular weight form a secondary peak centered at around 800 monomers (see figure insets), suggesting that at this low extent of reaction branched molecules are primarily formed by recombination of two macroradicals, each with an average length equal to that of the original distribution (i.e., 400 monomers). BP-BP results in a larger change in the height of the primary peak upon UV exposure, indicating that the overall extent of UV induced radical reactions in PS is higher for BP-BP than for BP. The increased overall radical activity of BP-BP, however, does not lead to more branching reactions but rather brings about an increase in main chain scission reactions as evidenced by the increased fraction of lower MW chains produced with BP-BP than with BP.

The chromatograms for the rubbery P*n*BA systems are shown in Figure 5. The effects of exposure time and photoinitiator equivalents are again similar: increasing exposure time has the same effect as increasing the photoinitiator equivalents. From the top two graphs in Figure 5, it is clear that BP-BP is significantly more efficient in initiating radical reactions than is BP. The increased radical activity seen in BP-BP is manifest as an increase in higher molecular weight, branched polymers. In comparison to what was seen in PS, the lower molecular weight regions of the chromatograms for P*n*BA show little to no change upon irradiation, indicating that main chain scission reactions do not occur for P*n*BA to any appreciable extent. The higher molecular weight branched molecules for P*n*BA again give rise to a subsidiary maximum at about twice the molecular weight of the original parent polymer due to recombination of two macroradicals; however, the chromatograms exhibit significant fractions of much higher molecular weight polymers that can arise only from higher order branching reactions involving recombination of previously branched macroradicals.

The chromatograms for rubbery P*n*BA are qualitatively different than those for glassy PS as is evident from the comparison of their chromatograms shown in Figure 6. The most obvious difference is that the extent of radical reactions is much higher for P*n*BA, a result that can partially be attributed to the much higher mobility of rubbery P*n*BA compared to glassy PS (note that for the data in Figure 6 the PS samples are irradiated 18 times longer than are the P*n*BA systems). It is also apparent that there is much less main chain scission for P*n*BA than for PS. BP-BP is more efficient than BP in inducing radical reactions for both PS and P*n*BA; however, the effect is much stronger for P*n*BA.

The overall extents of radical reactions for each experiment, estimated from the decrease in height of the primary GPC peak

dx.doi.org/10.1021/ma4007347 | *Macromolecules* 2013, 46, 5434−5444

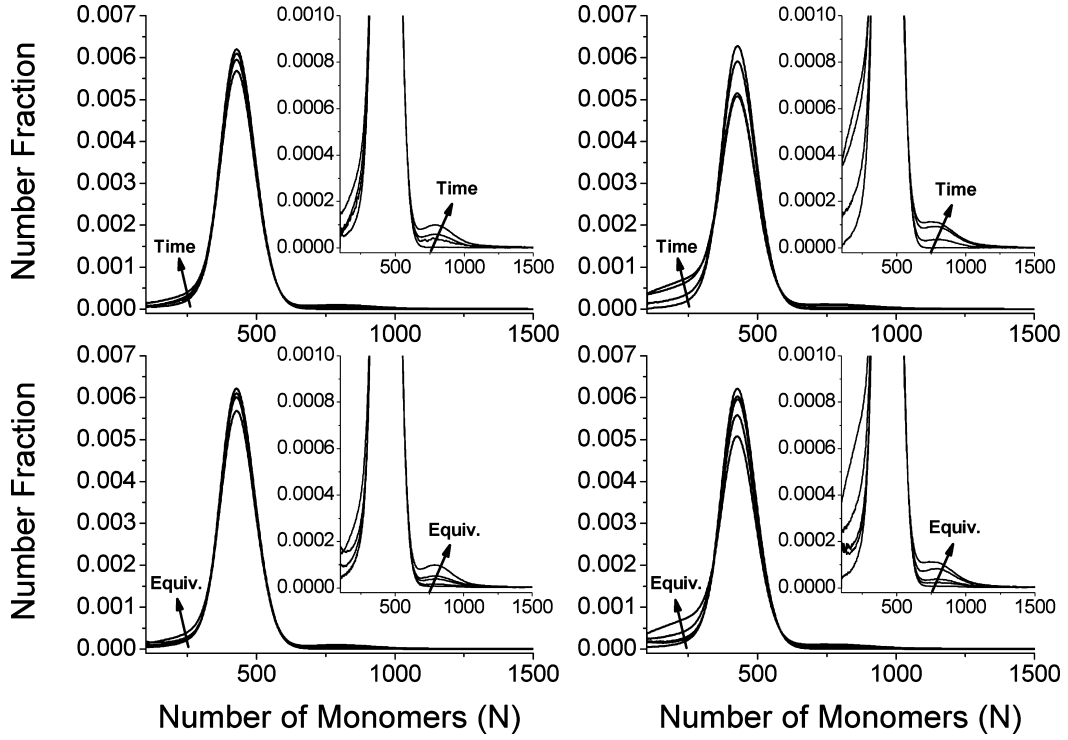

Figure 4. GPC chromatograms for PS upon exposure to UV radiation in the presence of BP (figures on left) and BP-BP (figures on right). The top figures show the effect of UV exposure time at a fixed photoinitiator content of 32 equiv. The bottom figures show the effect of photoinitiator content (i.e., equivalents) at a fixed UV exposure time of 9 h. The insets show the data on an expanded scale.

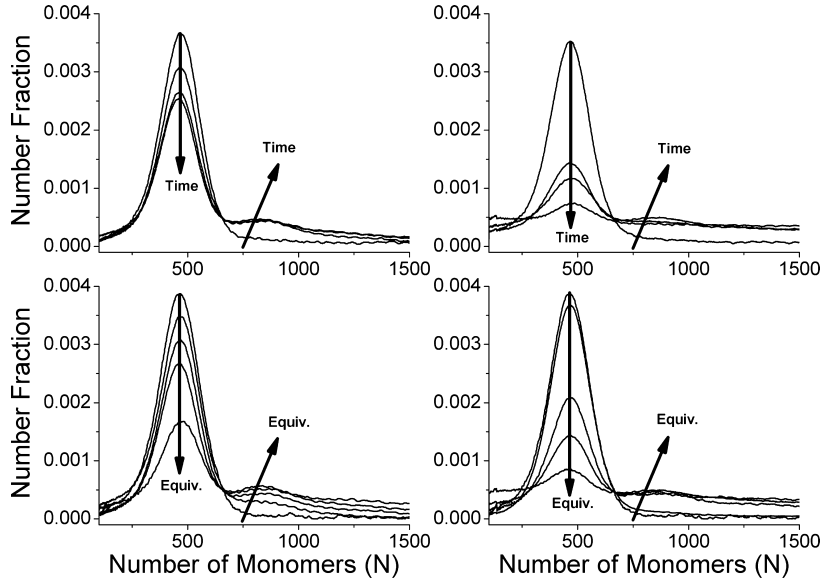

Figure 5. GPC chromatograms for P*n*BA1 upon exposure to UV radiation in the presence of BP (figures on left) and BP-BP (figures on right). The top figures show the effect of UV exposure time at a fixed photoinitiator content of 2.4 equiv. The bottom figures show the effect of photoinitiator content (i.e., equivalents) at a fixed UV exposure time of 3 h.

after UV exposure, are shown in Table 1. Because the propensity for polymer radical reactions is directly proportional to the number of radicals formed, it can be concluded that the total number of radicals formed follows the order P*n*BA/BP-BP > P*n*BA/BP > PS/BP-BP > PS/BP. Finally, although BP-BP induces more scission reactions (i.e., lower MW fragments) for P*n*BA than does BP, the two photoinitiators cause relatively little MW reduction in P*n*BA and a much larger relative extent of branching than was seen for PS.

DISCUSSION

Bifunctional BP-BP was found to be a more efficient photoinitiator for promoting radical reactions than monofunctional BP, both for glassy PS and for rubbery P*n*BA. BP-BP was almost twice as effective as BP in PS and was more than 3 times more effective in P*n*BA. The higher efficiency for BP-BP to promote radical reactions also indicates that, at an equal number of photoinitiator equivalents, BP-BP produces more radicals than does BP. To understand the higher efficiency of BP, we begin by

dx.doi.org/10.1021/ma4007347 | *Macromolecules* 2013, 46, 5434−5444

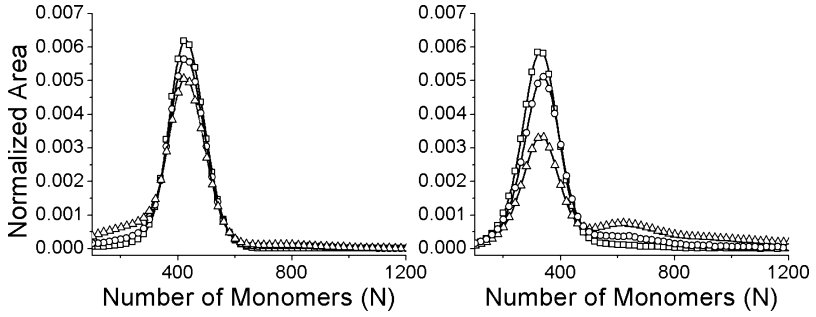

Figure 6. Comparison of GPC chromatograms for PS (left) and P*n*BA2 (right): controls without photoinitiator (squares); 32 equiv of BP (circles; 30 min for P*n*BA2 and 9 h for PS); 32 equiv of BP-BP (triangles; 30 min for P*n*BA2 and 9 h for PS).

Table 1. Percentage of Original Chains Involved in Radical Reactions

	% chains reacted	
sample	BP	BP-BP
PS (9 h)	9.79	15.66
P*n*BA (3 h)	20.28	62.94

examining the factors that influence the reactions associated with radical formation and how these factors differ between BP and BP-BP.

The first step in the process of radical generation is UV excitation of the photoinitiator molecule to the triplet state by the two reactions shown in Figure 2. While the mechanism of radical formation is identical for the two photoinitiators, the excitation wavelengths and extinction coefficients are different (see Supporting Information). Spectroscopic experiments (see Supporting Information) on BP and BP-BP demonstrate that BP-BP has a slightly higher absorbance at longer wavelengths and irradiation creates about 40% more excited states in BP-BP than in BP. The enhanced activity of BP-BP is a result of the electron-withdrawing effects of the ester group adjacent to each chromophore. The differences in chromophore activity alone, however, cannot account for the entire difference in efficiency between BP and BP-BP. The efficacy of BP-BP in P*n*BA is about 3 times higher than that of BP (see Table 1), whereas enhanced chromophore activity accounts for an increase in efficiency of only about 40%.

The second step in radical formation is abstraction of a proton from the polymer backbone by the excited chromophore. The efficiency of this reaction is affected by a number of factors, most importantly, the concentration of excited state chromophores and the mobility of the reactants. An important phenomenon that can affect the concentration of excited state chromophores is self-quenching of excited photoinitiator chromophores. Self-quenching occurs when two chromophores in the excited state come into close enough proximity to exchange energy and decay back to the ground state. Self-quenching reduces the concentration of excited chromophores and thereby lowers the overall photoinitiator efficiency.

The probability of self-quenching increases with molecular mobility and with the square of the concentration of excited chromophores. Studies on penetrant diffusion in polymers have shown that the diffusion coefficient of the penetrant scales inversely with its size. The mobility of BP is therefore considerably higher than that of BP-BP because it is less than half its size. While higher chromophore mobility translates into a higher degree of quenching, it is also expected to increase the rate of radical formation by the hydrogen abstraction reactions illustrated in Figure 2 and in the Supporting Information. The net influence of mobility on the photoinitiator efficiency is therefore not clear: the former effect decreases the excitation efficiency while the latter effect increases the rate of radical formation. Self-quenching is also enhanced by aggregation processes such as crystallization and phase separation. We have found that BP is more prone to these aggregation processes than is BP-BP due to its higher mobility and symmetry (see Supporting Information) but have minimized aggregation effects by appropriate sample preparation. The concentration of BP-BP molecules at equal number of photoinitiator equivalents is half that of BP because of the inclusion of 2 equiv of photoinitiator in each BP-BP molecule. Since the probability of two excited chromophores meeting each other scales with the square of the concentration, the probability of BP self-quenching is expected to be about 4 times greater than that of BP-BP. In addition, the rigidity of the linkage between the two chromophores in BP-BP causes steric hindrance that inhibits intramolecular self-quenching and may also impede intermolecular self-quenching. The higher efficiency of BP-BP for producing radicals relative to BP can therefore be attributed primarily to its lower probability for self-quenching.

Once a macroradical has formed, side reactions can occur that further differentiate the overall efficacy of BP-BP and BP, as depicted in Figure 7. We use the term backbone bonding to refer to reactions between a photoinitiator radical and a macroradical located on the chain backbone. If a BP radical reacts with a macroradical, a dead polymer with an attached BP is produced while one macroradical and one BP molecule are consumed. If a BP-BP monoradical reacts with a macroradical, a dead polymer

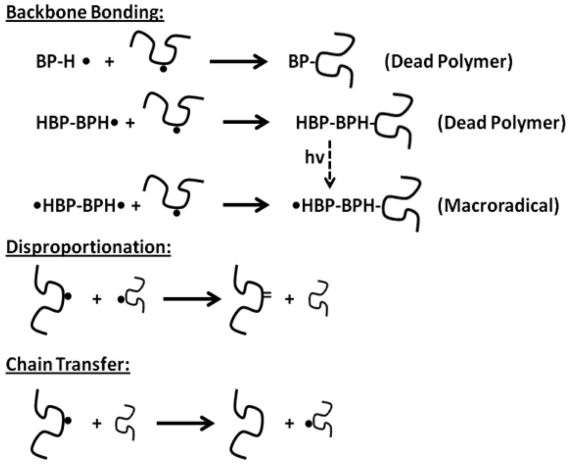

Figure 7. Macroradical side reactions.

dx.doi.org/10.1021/ma4007347 | *Macromolecules* 2013, 46, 5434−5444

with BP-BP attached is produced, consuming one of the chromophores; however, the second chromophore can be excited by a subsequent photon, and further radical reactions leading to a covalent bridge can ensue. If a BP-BP diradical bonds with a macroradical, two radicals annihilate, but the result is still a macroradical because one radical remains on BP-BP. Reactions of BP-BP radicals with a macroradical therefore reduce the number of BP-BP radicals by one in the system but conserve the number of macroradicals. The resultant BP-BP macroradical can react either with another macroradical to form a branched polymer bridged by a BP-BP linkage (see Figure 3) or with another BP-BP, the latter as a type of chain extension reaction. These bridging and extension reactions are only possible with BP-BP and furnish an additional explanation for the higher efficiency of BP-BP in producing branched polymers.

Macroradicals are also involved in chain transfer and disproportionation reactions, as shown in Figure 7. Chain transfer involves relocation of a radical from one molecule to another, so that the total number of radicals in the system is conserved. Disproportionation, in which two macroradicals react to produce a macromolecule with a double bond and a so-called dead macromolecule, consumes two macroradicals. The mechanisms of these side reactions are identical for BP and BP-BP and so have no influence on their relative activities.

The increased efficiency of the BP-BP photoinitiator compared to BP for promoting radical reactions can therefore be attributed to three effects: a 40% increase in the intrinsic efficiency of the chromophore, a lower probability of self-quenching, the latter by a factor as high as 4, and the possibility of bridging and chain extension reactions that cannot occur for BP.

A second distinction between BP-BP and BP that can account for differences in their cross-linking behavior is the spatial distribution of chromophores. Because the combination and side reactions under consideration are second-order under diffusion control, the reaction kinetics will depend on the distance between the two reactants involved in a particular reaction. As a first approximation, the average distance between photoinitiators can be determined by adoption of a simple cubic lattice model in which the lattice volume is set equal to the volume of one benzophenone moiety. To preserve equal benzophenone equivalents in the lattice, twice as many BP molecules as BP-BP molecules are required. This doubling of the molar density corresponds to a $2^{1/3}$ linear scaling of the lattice, as shown in Figure 8. As the number of equivalents increases, the linear distance between additive molecules, d_{BP} or d_{BP-BP}, becomes less and less differentiated. With 1 equiv, the linear distance between BP molecules is 6.39 lattice sites and the distance between BP-BP molecules is 8.05 lattice sites. At 32 equiv, the linear distance between BP molecules is 2.01 lattice sites while that between BP-BP molecules is 2.54 lattice sites. Differences in the behavior between BP and BP-BP that arise from the effects of spatial distribution will therefore be accentuated at low equivalents and should gradually disappear as the number of equivalents increases.

Figure 9 illustrates this trend by plotting the distances between chromophores as a function of the number of benzophenone equivalents. If we do not consider fluctuations and place the chromophores on a regular, repeating lattice, there is only one interchromophore distance for the BP system, which is equivalent to the intermolecular distance. In contrast, there are multiple interchromophore distances for the BP-BP system: the lattice dimension, that is, the distance between two adjacent chromophores on the same molecule, and a number of distances

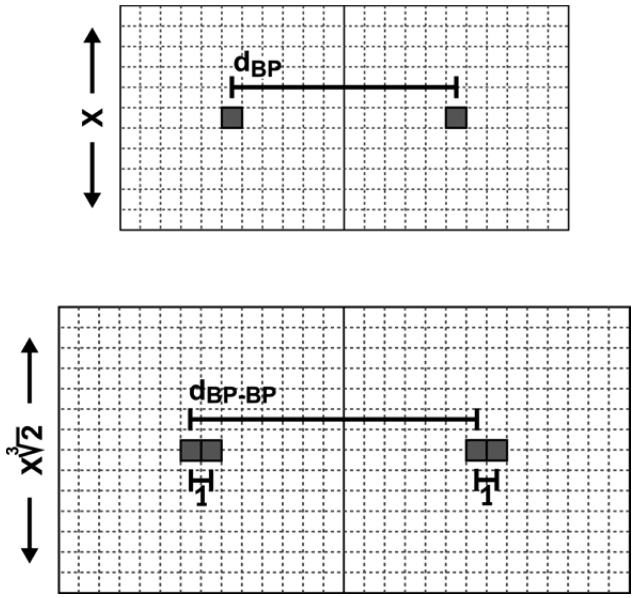

Figure 8. Projected lattices for BP (top) and BP-BP (bottom) for 1 equiv.

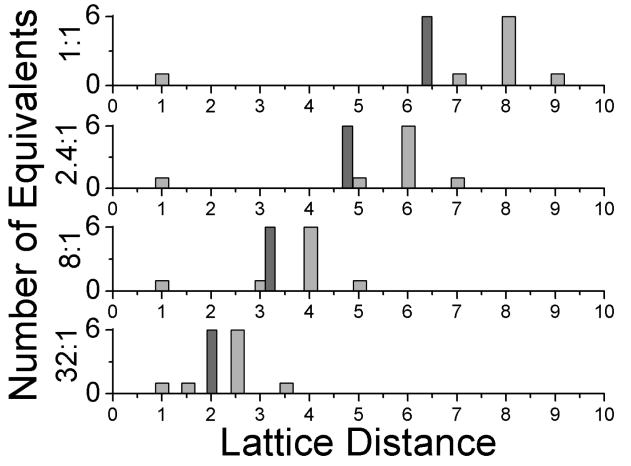

Figure 9. Distribution of distances between benzophenone chromophores for BP-BP (light gray bars) and BP (dark gray bars) as a function of the number of chromophore equivalents.

that depend on the relative orientation of the two photoinitiators. Only the primary distances are shown for BP-BP. The majority of the distances for BP-BP mirror those for BP when adjusted by the factor $2^{1/3}$ required to keep the number of benzophenone equivalents constant. Correlated side bands are present for BP-BP due to the bifunctionality of the additive. As the number of equivalents increases, the linear distance between species decreases until the spatial distributions of monofunctional and bifunctional additives are nearly equivalent. The effects of differences in spatial distribution between BP and BP-BP are therefore expected to be largest at low chromophore equivalents and gradually disappear with increase in the equivalents.

A complete description of the products produced in either the BP or BP-BP systems would require a detailed kinetic modeling of all of the reactions involved: chromophore excitation, macroradical formation, recombination, chain transfer, scission, and disproportionation. Such modeling, if even possible, is beyond the scope of this investigation. As an alternative, we can examine the relative importance of each of the reactions and the

dx.doi.org/10.1021/ma4007347 | *Macromolecules* 2013, 46, 5434−5444

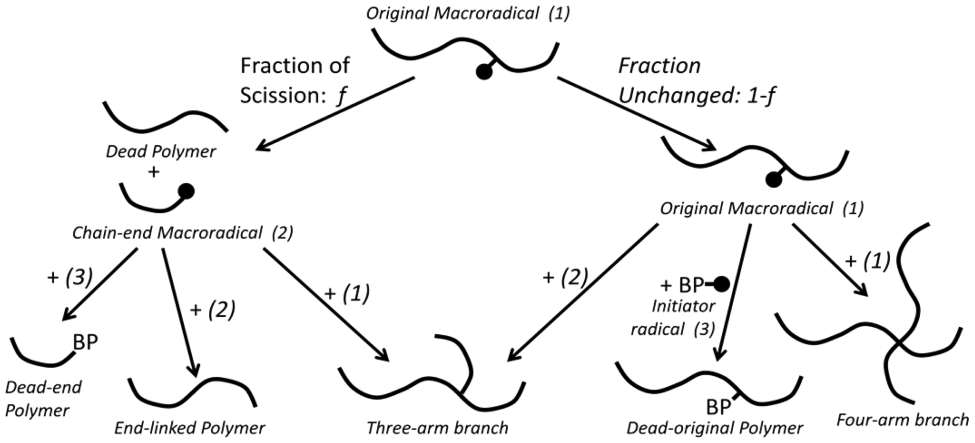

Figure 10. The fate of macroradicals: radical recombination reaction pathways. The fraction of macroradicals undergoing scission is *f*. The three reactive radical species are (1) the original macroradical, (2) a chain-end macroradical formed by scission, and (3) a photoinitiator radical.

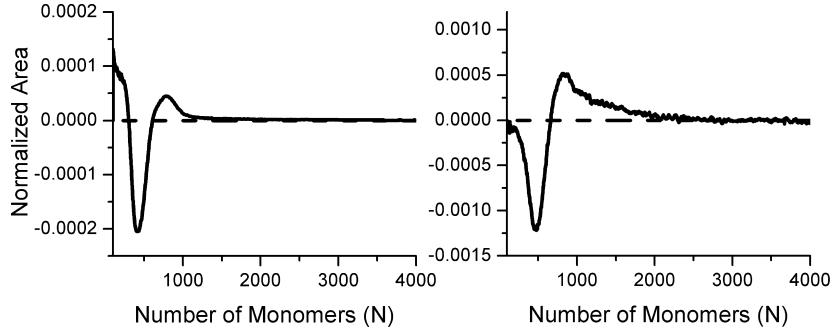

Figure 11. Typical normalized difference chromatograms used to separate the contributions of scission and chain branching reactions for benzophenone at 8 equiv: PS-9 h (left) and P*n*BA-3 h (right). The fraction of chains undergoing main chain scission is represented by the area under the curve to the left of the first zero crossing. The fraction of chains undergoing chain branching is represented by the area under the curve to the right of the second zero crossing. The central region of the difference spectrum is negative because the number of original chains decreases upon scission and branching. Note: the scale of the ordinate axis on the right graph is 6 times larger than that of the left graph.

likelihood of each product formation by taking a simple probabilistic approach. As the mobility of each of the reactants is not known, the effects of mobility will be ignored as a first approximation whereupon the probabilities for each reaction will be simply related to concentrations. The problem reduces to tracking the fate of the initial macroradical formed by the hydrogen abstraction reactions in Figure 2. The possible macroradical reactions for the BP systems are depicted in Figure 10. There are three reactive radical species: the original macroradical (1), a chain-end macroradical resulting from main chain scission (2), and a photoinitiator radical (3). The relative fraction of macroradicals that undergo main chain scission is denoted as *f*, and the relative fraction of remaining original macroradicals is $1 - f$.

The main chain scission reaction produces a chain-end macroradical and a dead polymer, denoted as dead-end polymer. The dead polymer chains cannot undergo further radical reactions unless they are reactivated by some reaction that would convert them back into a macroradical. The reactive radical species therefore are a mixture containing a fraction *f* of chain end macroradicals and a fraction $1 - f$ of original macroradicals and photoinitiator radicals of relative concentration that we denote as φ_{PR}. All of these radicals can undergo a number of radical recombination reactions.

In order to calculate the probabilities, *P*, of each reaction, we assume that the probabilities of finding an original macroradical (1), a chain-end radical (2), and a photoinitiator radical (3) are proportional to $[1 - f]$, *f*, and φ_{PR}, respectively. The probability of a chain-end macroradical (2) reacting with another chain-end macroradical (2) to form an end-linked linear polymer is therefore $P_{\text{end-linked}} \sim f^2$. The chain-end macroradical (2) can also react with a photoinitiator radical (3) to form dead-end polymer ($P_{\text{dead-end}} \sim \varphi_{PR} f$) or with an original macroradical to form a three-arm branched macromolecule ($P_{3\text{-star}} \sim [1 - f]$). The original macroradical (1) can react with another original macroradical (1) to form a four-arm branched macromolecule ($P_{4\text{-star}} \sim [1 - f]^2$), with a photoinitiator radical (3) to form a different dead polymer denoted as the dead-original polymer ($P_{\text{dead-original}} \sim \varphi_{PR}[1 - f]$) or with a chain-end macroradical (2) to form a three-arm branched macromolecule ($P_{3\text{-star}} \sim f[1 - f]$). The non-normalized probabilities for dead polymer formation are therefore of order $O \propto \varphi_{PR} f$ while those for all other species formed are of order $O \propto f^2$.

The BP-BP systems have the same reactions and probabilities as those for the BP systems with the exception of the additional chain extension and bridging reactions discussed previously. Because these latter reactions involve more than two components, however, their probabilities are necessarily lower than those associated with binary reactions. For example, the probability that two macromonomers are bridged by one BP-BP molecule to form the four-arm branch depicted at the bottom of Figure 3 is $P_{1\text{-bridge}} \sim \varphi_{PR}[1 - f]^2$, and the probability of forming a four-arm branch containing two BP-BP molecules would be $P_{2\text{-bridge}} \sim \varphi_{PR}^4[1 - f]^2$. The probabilities for branches forming by

dx.doi.org/10.1021/ma4007347 | *Macromolecules* 2013, 46, 5434−5444

bridging and chain extension reactions are therefore $O \propto f^4$ and higher and appreciably smaller than those formed by bimolecular combination reactions. The bridging reactions can normally be ignored and only become important when the fraction of initiator radicals becomes very large, that is, at high chromophore equivalents. The simple probabilistic approach indicates that, under normal circumstances, the structure of the photoinitiator is not important: the cross-linking reactions and their probabilities are identical for the BP and BP-BP systems.

The relative contribution of each of the radical reactions was evaluated by separating the chromatograms into three distinct components, each associated with specific radical mechanisms: molecules that suffered a decrease in molecular weight due to main chain scission, molecules with increased molecular weight due to chain branching, and molecules that were not affected by UV irradiation and retained their original molecular weight. Because each of these contributions is represented by a distribution of molecular weights and these distributions overlap, we developed an approximate separation procedure that is described in Figure 11. Each chromatogram (i.e., for a particular number of chromophore equivalents and a specific radiation time) was manipulated to produce an abscissa that is linear in degree of polymerization using, when appropriate, Mark–Houwink–Sakurada parameters, GPC calibration curves, and binning algorithms. We assumed that the fraction of low molecular weight fragments formed that fall below the detection limit of GPC was negligible so that the distribution could be normalized to an area of unity. The normalized MWD of the control was then subtracted from each of these normalized chromatograms to produce a difference chromatogram. The three regions of behavior are then taken as the regions defined by the zero crossings as illustrated in the figure.

The relative contributions of main chain scission and chain branching reactions as determined by the parsing procedure illustrated in Figure 11 are shown in Figures 12–14 for PS scission, PS combination, and P*n*BA and P*n*BA2 combination, respectively. While there are a few outliers, from Figures 12 and 13 it is evident that in the PS thin films the fraction of chains undergoing chain branching is the same for the BP and BP-BP systems but that the degree of main chain scission is higher in the

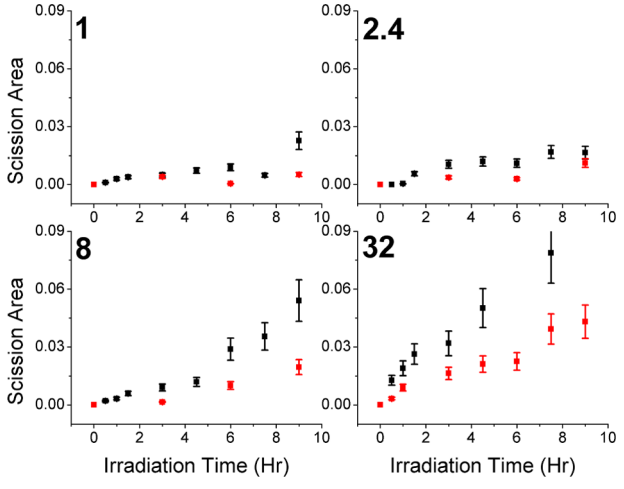

Figure 12. PS scission areas in BP (red) and BP-BP (black) systems with irradiation time at 4 equiv: 1, 2.4, 8, and 32. Error bars are the standard deviation of nine runs of a single model system and are equal to 20% of the datum value. All axes are equal.

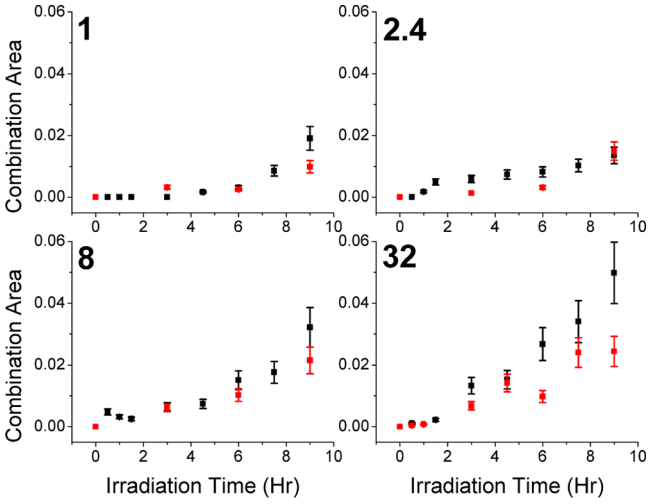

Figure 13. PS combination areas in BP (red) and BP-BP (black) systems with irradiation time at 4 equiv: 1, 2.4, 8, and 32. Error bars are the standard deviation of nine runs of a single model system and are equal to 20% of the datum value. All axes are equal.

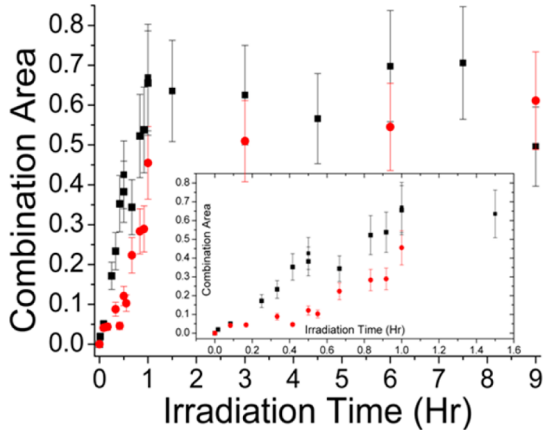

Figure 14. P*n*BA combination data for P*n*BA2 and BP (red) and P*n*BA2 and BP-BP (black), both at 32 equiv. The inset is a magnification of the results at low time to illustrate the difference in slopes. Error bars are the standard deviation of nine runs of a single model system and are equal to 20% of the data value.

BP-BP systems than in the BP systems. It was shown earlier that BP-BP is more effective in producing macroradicals than is BP; however, the data in Figures 12 and 13 demonstrate that this added efficiency does not result in more branching, but rather leads to more main chain scission, except at high equivalents as discussed earlier.

An explanation for this result must lie in the three intrinsic differences between the two photoinitiators: (1) BP has a higher mobility than BP-BP due to its smaller size; (2) BP-BP is more efficient in producing macroradicals, and (3) the BP-BP molecules are farther apart at equal equivalents. The first factor should be relatively unimportant because branching occurs by recombination of macroradicals and the mobility of macroradicals is not affected significantly by the mobility of the photoinitiators. The second factor would increase both chain branching and scission, if the spatial distribution of macroradicals were the same in the BP and BP-BP systems; however, the third factor would cause relatively more branching in the BP system, since the distance between macroradicals is smaller. Scission

dx.doi.org/10.1021/ma4007347 | *Macromolecules* 2013, 46, 5434–5444

becomes more favorable with increased distance between macroradicals because the longer time required for two macromonomers to form a branch by recombination allows for more scission. Considering all three factors, it is clear that there should be more scission in the BP-BP system than in the BP system because there are more macroradicals in the former. The situation regarding branching is not as clear because the BP-BP system has more radicals, increasing the probability of branch formation, but the distance between BP-BP molecules is greater so that the rate of branching should be lower for BP-BP. The data suggests that these two factors counteract each other as the degree of branching in the BP and BP-BP systems was found to be the same. Figure 13 shows that at high equivalents (i.e., 32) the close distance between BP-BP molecules begins to overcome the probabilistic deterrence to bridging and BP-BP becomes more efficient in cross-linking than BP.

Polymer mobility has a direct influence on the effectiveness of the photoinitiators. In PS, the branching reactions observed under the conditions employed produced mostly bimolecular branching reactions that effectively doubled the average molecular weight. In contrast, branched molecules with molecular weights of more than 10 times the original were found for P*n*BA, indicating significant amounts of higher order branching reactions. The rates of the radical reactions are also considerably faster in P*n*BA than in PS. As shown in Table 1, BP and BP-BP induce 3−4 times more radical reactions in P*n*BA as in PS in only one-third the amount of time. Because P*n*BA is a rubber at experimental temperatures, bulk chain motion is feasible and two macroradicals can diffuse together by either short- or long-range motion. In the glassy PS systems, macroradicals can move and react only through short-range sub-T_g motions such as that of the β-transition which are highly constrained spatially. Fundamentally, the lower mobility has two basic effects: first, it increases the time required for radical formation by hydrogen abstraction which increases the time available for decay of the excited photoinitiator back to the ground state and thereby decreases the number of macroradicals formed; second, it increases the time required for macroradical recombination, leading to a higher degree of main chain scission.

The P*n*BA combination reaction areas, shown in Figure 14, reach a plateau after a few hours of irradiation, indicating either that the additives have been completely reacted, which is unlikely, or that the P*n*BA has gelled and we are measuring the MWD of only the sol fraction that is extractable from the irradiated thin films. The fact that we detect very large P*n*BA molecules supports the latter conclusion. In fact, we have recently shown that these photoactive additives can be used to photochemically generate gels from preformed polymers.[25]

Little to no scission is visible in the P*n*BA systems (see Figures 5 and 6), whereas the PS systems exhibited appreciable scission that increased with the irradiation time, the number of chromophore equivalents, and the photoinitiator functionality. The mobility argument properly predicts that the probability of scission should be higher in the less mobile PS than in the more mobile P*n*BA; however, we believe an alternative argument is the primary origin of this difference.

The structures of the PS and P*n*BA monomers, shown in Figure 15, indicate the locations of all hydrogen atoms. The bond dissociation energy of the C−H bond to be abstracted must be below 427 kJ/mol for the hydrogen abstraction reaction to occur (see Supporting Information). In the PS monomer, the bond dissociation energy of the phenyl hydrogens, 474.8 kJ/mol,[27] is considerable higher than those of the secondary and tertiary

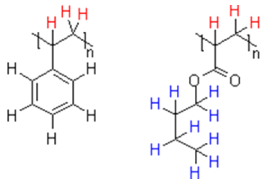

Figure 15. A comparison of abstractable hydrogen atoms for PS (left) and P*n*BA (right). The red hydrogen atoms are on the chain backbone, and the blue hydrogen atoms are on the side chains.

backbone hydrogens, 410.2 and 348.1 kJ/mol,[27] respectively. Hydrogen abstraction therefore occurs primarily on chain backbone carbons, marked red in Figure 15; however, abstraction can be sterically inhibited by rotations of the phenyl ring that shield backbone carbon atoms. For P*n*BA, there are five types of hydrogen atoms: tertiary on the backbone (388.3 kJ/mol[27]), secondary on the pendant group next to the oxygen(392.1 kJ/mol[27]), secondary on the backbone (410.2 kJ/mol[27]), secondary on the pendant group (411.1 kJ/mol[27]), and primary on the pendant group (421.3 kJ/mol[27]). For P*n*BA, the backbone hydrogens are red and the pendant hydrogens are blue in Figure 15. Hydrogen abstraction is favored for the lowest energy tertiary hydrogen on the backbone, but the high flexibility and mobility of the pendant group above T_g sterically shield the backbone hydrogens from the excited chromophore so that hydrogen abstraction is expected to occur primarily on the pendant side chain. β scission due to radicals on the pendant side chains does not cause main chain scission and therefore does not lead to significant molecular weight changes because the short pieces of pendant groups cleaved are below the resolution limit of the GPC. These considerations indicate that branches form in PS by recombination of chain backbone radicals while branches form in P*n*BA primarily by recombination of radicals on pendant side chains.

The differences observed between the branching behavior of PS and P*n*BA suggest a design philosophy that allows for the isolation of desired effects and the negation of undesirable reactions. A polymer with an easily accessible pendant group or easily abstractable hydrogen on the same will preferentially form radicals at that location and the probability of backbone radicals will be diminished, possibly to zero. That system, in the presence of hydrogen abstracting materials or materials that rely on other chemistries, will generate branches without appreciable main chain scission. Cross-linking systems with too much scission can be modified by using an equivalent polymer with easily abstractable hydrogen atoms located on pendant side chains. Poly(4-methylstyrene), for example, should provide the benefits of polystyrene with significantly reduced main chain scission and is currently under study.

If the additives are assumed to create a macroradical at their location upon excitation, then the location of the macroradicals in the system will be equivalent to the location of the additive molecules. Once formed, two macroradicals must come together to react and form a branch point. This reaction, assuming standard kinetics, will progress at the following rate:

$$\text{rate}_{\text{combination}} = \frac{dC_{\text{combination}}}{dt} \approx kC^2_{\text{macroradicals}} \approx kC^2_{\text{additive}} \quad (1)$$

where C is the concentration of the subscripted species and t is time. If, on the other hand, the reaction is diffusion-controlled, then the diffusion of the additives or macroradicals will be the key

dx.doi.org/10.1021/ma4007347 | *Macromolecules* 2013, 46, 5434−5444

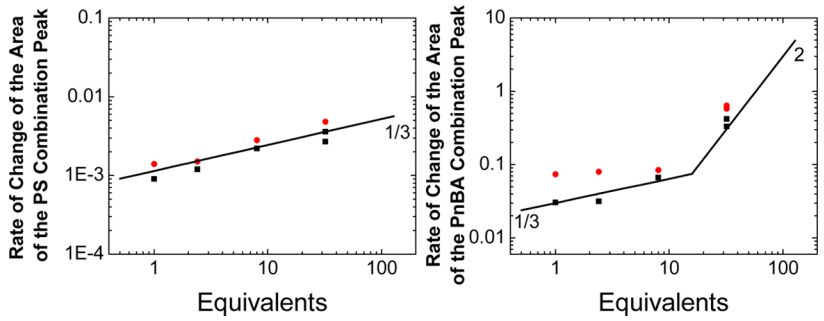

Figure 16. Rate of change of the combination areas with time in PS (left) and P*n*BA (right) with photoinitiators BP (black squares) and BP-BP (red circles) plotted against the equivalent concentration in log−log space. Lines are arbitrarily located and have slopes as marked.

to the kinetics of branch formation. For a diffusion-controlled reaction, rate $\propto \mathcal{D}t^{1/2} = \mathcal{D}^{1/2}\sqrt{\mathcal{D}t}$, where $\mathcal{D}$ is the diffusion constant and ($\sqrt{\mathcal{D}t}$ is a characteristic distance, which, in our system, is the linear distance between additive molecules or macroradicals. The linear distance between additive molecules (and the macroradicals they produces) is proportional to their bulk concentration to the one-third power. The rate of branch formation in a diffusion controlled system will therefore progress as

$$\text{rate}_{\text{combination}} = \frac{dC_{\text{combination}}}{dt} \approx \mathcal{D}^{1/2} C_{\text{macroradicals}}^{1/3} \approx \mathcal{D}^{1/2} C_{\text{additive}}^{1/3} \quad (2)$$

Equations 1 and 2 allow us to determine whether our systems are under diffusion or kinetic control. Figure 16 shows a log−log plot of the rate of branch formation ($\text{rate}_{\text{combination}}$) against the concentration in equivalents (C_{additive}). It includes arbitrarily lines with slopes of 1/3 and 2 to compare the data to eqs 1 and 2. In the PS system, diffusive processes dominate as would be expected in a glassy thin film where only slow short-range motions of macroradicals are feasible. For P*n*BA, diffusion control is expected at low equivalent concentrations when the inter-radical distances are too large to allow for recombination through bulk chain motion. At high equivalents in P*n*BA, the data show suggest that the transition to kinetic control may be occurring as the rate scales with a much higher power of concentration approaching the value of two expected for kinetic control. Unfortunately, the accuracy of the data is not sufficient to prove this transition. It can be concluded that over the range of parameters studied that the rates of recombination in both PS and P*n*BA are controlled primarily by diffusion. The fact that the rates of combination observed for PS and P*n*BA differ only by a factor on the order of 10^3 can be taken as indication that most recombination reactions occur by short-range motion of macroradicals in both systems, as the difference in the rate of bulk chain diffusion between glassy PS and rubbery PnBA is much larger than this factor.

CONCLUSIONS

Preformed polymers can be branched/cross-linked even in the glassy state by irradiation of incorporated bis-benzophenone (BP-BP) and benzophenone (BP) photoinitiator. BP-BP is more efficient than BP for inducing radical reactions due to a combination of effects associated with differences in their intrinsic chromophore properties, their mobility, their accessible side reactions, and their spatial distribution. The polymer matrix determines in large part the fate of the additional radicals formed with BP-BP. In glassy polystyrene, bifunctional additives do not provide additional chain branching reactions, except at high additive concentration where the probability of bridging reactions becomes significant, and instead lead to additional main chain scission reactions, an undesirable result. In contrast, little evidence of main chain scission is found for rubbery poly(*n*-butyl acrylate) with either additive, and BP-BP leads to more chain branching reactions than does BP. Such markedly different behavior for different polymers is due to the fact that the location of radical formation is highly dependent on the molecular structure of the polymer. In the case of PS, radicals can only form by hydrogen abstraction on the chain backbone such that radical scission reactions lead to breakage of the main chain and the formation of low molecular weight fragments. In the case of P*n*BA, radicals form primarily on the side chains such that radical scission reactions due not cause main chain breakage and cause little change in molecular weight. The mobility of the polymer also plays a role, as the rates of recombination leading to branching are found to be significantly higher in the rubbery P*n*BA.

ASSOCIATED CONTENT

Supporting Information

Synthesis of the bifunctional benzophenone, the hydrogen abstraction mechanism in our system, the data analysis methodology, the photochemical properties of the systems and materials used, relevant macroradical kinetic constants, local and bulk aggregation and crystallization effects in the samples, the control systems, a comment on the glass transition temperature, and EPR experiments. This material is available free of charge via the Internet at http://pubs.acs.org.

AUTHOR INFORMATION

Corresponding Author

*E-mail jk1191@columbia.edu (J.T.K.).

Notes

The authors declare no competing financial interest.

ACKNOWLEDGMENTS

This material is based upon work supported by the National Science Foundation under grant DMR-0704054. J.R.L. and N.D.C. were partially supported by fellowships provided by National Science Foundation grant IGERT-0221589.

REFERENCES

(1) Tillet, G.; Boutevin, B.; Ameduri, B. *Prog. Polym. Sci.* **2011**, *36*, 191−217.

(2) Barkalov, I. M. In *Advances in Interpenetrating Polymer Networks*; Klempner, D., Firisch, K. C., Eds.; Technomic: Lancaster, PA, 1991; Vol. *II*, pp 1−23.
(3) Rouif, S. *Radiat. Phys. Chem.* **2004**, *71*, 527−530.
(4) Morrison, N. J.; Porter, M. *Rubber Chem. Technol.* **1984**, *57* (1), 63−85.
(5) Krejsa, M. R.; Koenig, J. L. *Rubber Chem. Technol.* **1993**, *66* (3), 376−410.
(6) Hulse, G. E.; Kersting, R. J.; Warfel, D. R. *J. Polym. Sci., Polym. Chem.* **1981**, *19* (3), 655−667.
(7) Brostow, W.; Datashvili, T.; Hackenberg, K. P. *Polym. Compos.* **2010**, *31* (10), 1678−1691.
(8) Chen, Z.; Liu, Z.; Liu, F.; Yang, L. *Zhongguo Shengwu Gongcheng Zazhi* **2003**, *23* (4), 99−101−105.
(9) DeSantis, G.; Jones, J. B. *Curr. Opin. Biotechnol.* **1999**, *10* (4), 324−330.
(10) Guilbault, G. G. *Bio/Technology* **1989**, *7* (4), 349−51.
(11) Jayakrishnan, A.; Jameela, S. R. *Biomaterials* **1996**, *17* (5), 471−84.
(12) Lin, L.; Tang, Y.; Chang, R.; Zhou, J.; Cui, J.; Hu, S.; Zhang, F. *Zhongguo Yixue Kexueyuan Xuebao* **2003**, *25* (6), 735−737.
(13) Xu, J.; Yuan, Z.; Zhang, Y.; Zhuang, X.; Xu, H.; Liang, C.; Ma, L. *Huagong Jinzhan* **2010**, *29* (3), 494−497.
(14) Doytcheva, M.; Stamenova, R.; Zvetkov, V.; Tsvetanov, C. B. *Polymer* **1998**, *39* (26), 6715−6721.
(15) Nagata, M.; Hizakae, S. *Macromol. Biosci.* **2003**, *3* (8), 412−419.
(16) Carroll, G. T.; Sojka, M. E.; Lei, X.; Turro, N. J.; Koberstein, J. T. *Langmuir* **2006**, *22* (18), 7748−7754.
(17) Allen, N. S.; Marin, M. C.; Edge, M.; Davies, D. W.; Garrett, J.; Jones, F.; Navaratnam, S.; Parsons, B. J. *J. Photochem. Photobiol., A* **1999**, *126* (1−3), 135−149.
(18) Koberstein, J. T.; Carroll, G.; Jahani, J.; Turro, N. J. *Polym. Prepr. (Am. Chem. Soc., Div. Polym. Chem.)* **2007**, *48* (1), 808.
(19) Doytcheva, M.; Dotcheva, D.; Stamenova, R.; Orahovats, A.; Tsvetanov, C.; Leder, J. *J. Appl. Polym. Sci.* **1997**, *64* (12), 2299−2307.
(20) Pappas, S. P. *Prog. Org. Coat.* **1974**, *2* (4), 333−47.
(21) Qu, B.; Xu, Y.; Ding, L.; Ranby, B. *J. Polym. Sci., Part A: Polym. Chem.* **2000**, *38* (6), 999−1005.
(22) Ruhe, J.; Madge, D. Abstracts of Papers, 225th ACS National Meeting, New Orleans, LA, March 23−27, 2003; PMSE-156.
(23) Ruhe, J.; Seidel, K.; Toomey, R. Abstracts of Papers, 227th ACS National Meeting, Anaheim, CA, March 28−April 1, 2004; COLL-358.
(24) Millan, M. D.; Locklin, J.; Fulghum, T.; Baba, A.; Advincula, R. C. *Polymer* **2005**, *46* (15), 5556−5568.
(25) Carroll, G. T.; Triplett, L. D.; Moscatelli, A.; Koberstein, J. T.; Turro, N. J. *J. Appl. Polym. Sci.* **2010**, 122.
(26) Beuermann, S.; Paquet, D. A.; McMinn, J. H.; Hutchinson, R. A. *Macromolecules* **1996**, *29* (12), 4206−4215.
(27) BDEs of C-H bonds. In *Comprehensive Handbook of Chemical Bond Energies*; Luo, Y., Ed.; CRC Press: Boca Raton, FL, 2007; pp 19−145.